



Two-step method for radiative transfer calculations in a developing pool fire at the initial stage of its suppression by a water spray

Leonid A. Dombrovsky^{a,b,c,*}, Siaka Dembele^a, Jennifer X. Wen^d, Ivan Sikic^d

^a Department of Mechanical & Automotive Engineering, Kingston University, London SW15 3DW, UK

^b Joint Institute for High Temperatures, 17A Krasnokazarmennaya St, Moscow 111116, Russia

^c The University of Tyumen, 6 Volodarsky St, Tyumen 625003, Russia

^d School of Engineering, University of Warwick, Coventry CV4 7AL, UK

ARTICLE INFO

Article history:

Received 25 May 2018

Received in revised form 16 July 2018

Accepted 17 July 2018

Keywords:

Radiation

Developing pool fire

Fire suppression

Water droplets

Computational method

ABSTRACT

A procedure based on two-step method is suggested to simplify time-consuming spectral radiative transfer calculations in open flames containing scattering particles. At the first step of the problem solution, the P_1 approximation is used to calculate the divergence of radiative flux, and it is sufficient to determine the flame parameters. The second step of solution is necessary to obtain the radiation field outside the flame, and this can be made independently using the ray-tracing procedure and the transport source function determined at the first step. Such a splitting of the complete problem results in much simpler algorithm than those used traditionally. It has been proved in previous papers that the combined two-step method is sufficiently accurate in diverse engineering applications. At the same time, the computational time decreases in about two orders of magnitude as compared with direct methods. An axisymmetric pool fire at the initial stage of fire suppression by a water spray is considered as the case problem. It is shown that evaporating small water droplets characterised by a strong scattering of infrared radiation are mainly located in regions near the upper front of the flame and one can observe the scattered radiation. This effect can be used in probe experiments for partial validation of transient Computational Fluid Dynamics (CFD) simulations.

© 2018 The Authors. Published by Elsevier Ltd. This is an open access article under the CC BY license (<http://creativecommons.org/licenses/by/4.0/>).

1. Introduction

Radiative transfer calculations are the most time-consuming in CFD simulation of fires. Therefore, the use of a simple but sufficiently accurate method for the radiative transfer is critically important to improve the computational costs of CFD codes. A numerical analysis of suppression of fires by water sprays is possible only with the use of spectral models because the optical properties of water droplets cannot be considered on the basis of a gray model [1]. In most cases, there is no need for a very detailed radiation field in CFD calculations. Only the total or integral (over the spectrum) radiative flux divergence is important because this term is needed in the energy equation that couples thermal radiation with other modes of heat transfer. It means that one can consider a differential approach instead of the radiative transfer equation (RTE). Such a choice is really reasonable in the case of combined heat transfer problems including those for fires and combustion

systems [1,2]. The P_1 (the first-order approximation of the spherical harmonics method) [1–4] is the simplest method of this type, and there is a very positive long-time experience of using this approach in diverse multi-dimensional problems [1,5–17]. It appears to be sufficiently accurate in the case when one needs only the divergence of radiative flux in the energy equation. Moreover, it was shown in recent paper [18] that the P_1 error is sometimes less than that of the finite-volume method.

It was demonstrated in early papers [19–21] that P_1 approximation may give incorrect values of radiative flux near the boundaries of the computational region in the case of a strong decrease of temperature or extinction coefficient of the medium towards the region boundaries. Unfortunately, this is the case for open flames. Therefore, the second step of the computational radiative transfer model is necessary. This can be done using the transport approximation [12] and a ray-tracing procedure for the RTE with the transport source function determined at the first step of solution. In particular, this combined two-step method presented in papers [5,19,20] was successfully employed in recent paper [17] to calculate radiative heat transfer from supersonic flow with suspended particles to a blunt body.

* Corresponding author at: Joint Institute for High Temperatures, 17A Krasnokazarmennaya St, Moscow 111116, Russia.

E-mail address: ldombro@yandex.ru (L.A. Dombrovsky).

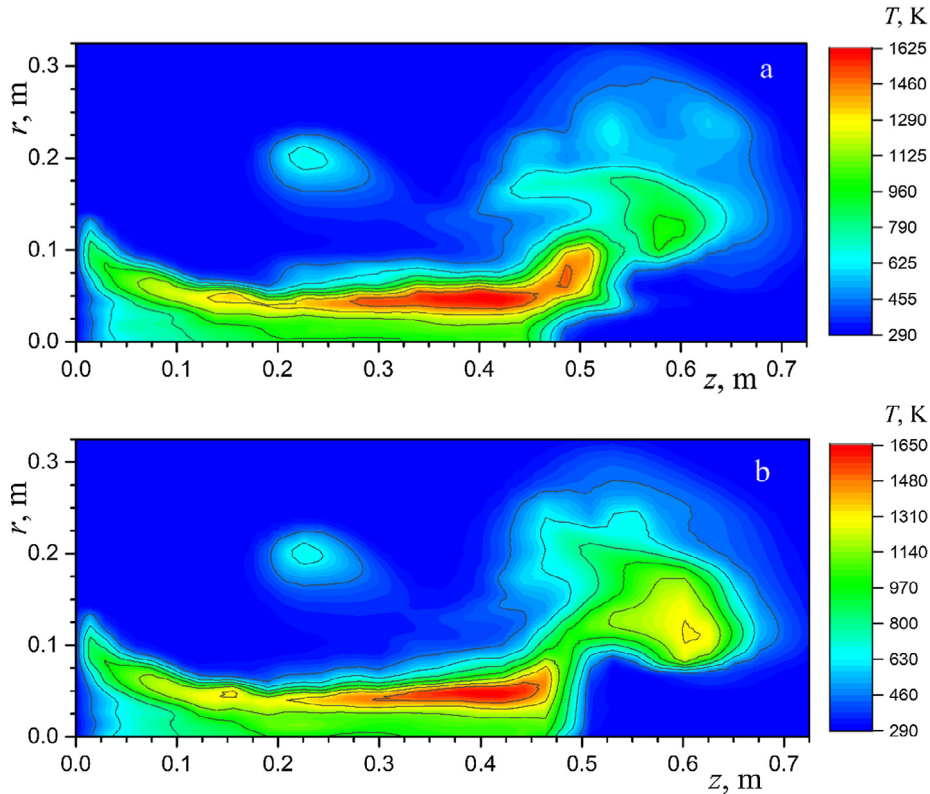


Fig. 1. The gas temperature field in the model flame: a – the calculation without account for thermal radiation, b – the complete calculation.

calculations. As to the radiative flux from the flame, it can be calculated using a ray-tracing procedure at the second step of solution independently of the CFD calculations.

3. Two-step method for radiative transfer calculations

The general theoretical model for transfer of thermal radiation in a flame should be based on the radiative transfer equation (RTE) which takes into account emission, absorption, and scattering of radiation in the medium. A special feature of the fire suppression problem is the anisotropic scattering of radiation by relatively cold water droplets. In this case, the RTE can be written as follows [1] (hereafter, we omit the subscript “λ” in the medium radiative properties for brevity):

$$\vec{\Omega} \nabla I_i(\vec{r}, \vec{\Omega}) + \beta I_i(\vec{r}, \vec{\Omega}) = \frac{\sigma}{4\pi} \int_{(4\pi)} I_i(\vec{r}, \vec{\Omega}') \Phi(\vec{\Omega}' \cdot \vec{\Omega}) d\vec{\Omega}' + \alpha_g I_b(T_g(\vec{r})) \quad (1)$$

The physical meaning of Eq. (1) is evident: variation of the spectral radiation intensity, I_i , in direction $\vec{\Omega}$ takes place due to self-emission of thermal radiation by gases (the last term, $I_b(T)$ is the Planck function), extinction by absorption and also by scattering in other directions (the second term), as well as due to scattering from other directions (the integral term). The spectral extinction coefficient β is a sum of the absorption coefficient, $\alpha = \alpha_g + \alpha_d$, (both gas and water droplets contribute to absorption) and the scattering coefficient, σ , of a conventional continuous medium of droplets. These spectral coefficients and the scattering phase function, Φ , depend on spatial coordinate \vec{r} .

The integration of RTE (1) over all values of the solid angle gives the following important expression for divergence of the spectral radiative flux [1]:

$$\nabla \vec{q}_\lambda = 4\pi\alpha_g I_b(T_g) - \alpha G_\lambda \quad (2)$$

which can be treated as a local balance of the spectral radiation energy. The spectral radiative flux and irradiation function are defined as follows:

$$\vec{q}_\lambda(\vec{\Omega}) = \int_{(4\pi)} I_\lambda(\vec{r}, \vec{\Omega}) \vec{\Omega} d\vec{\Omega} \quad G_\lambda(\vec{r}) = \int_{(4\pi)} I_\lambda(\vec{r}, \vec{\Omega}) d\vec{\Omega} \quad (3)$$

The first term in the right-hand side of Eq. (2) is the emission, whereas the second term is the radiation absorption by both the gases and water droplets.

A complete and accurate solution to the RTE in scattering media is a very complicated task. One can find many studies in the literature on specific numerical methods developed to obtain more accurate spatial and angular characteristics of the radiation intensity field. Several modifications of the discrete ordinates method (DOM), finite-volume method (FVM), and statistical Monte Carlo (MC) methods are the most popular tools employed by many authors (see [1–4] for the details). The main difficulty of accurate radiative transfer calculations is related with the angular dependence of radiation intensity. Fortunately, this angular dependence appears to be rather simple in many important applied problems. It enables one to use this property of solution to derive relatively simple but fairly accurate differential approximations.

All the differential approximations for RTE are based on simple assumptions concerning the angular dependence of the spectral radiation intensity I_λ . These assumptions enable us to deal with a limited number of functions $I_\lambda^i(\vec{r})$ instead of function $I_\lambda(\vec{r}, \vec{\Omega})$ and turn to the system of the ordinary differential equations by the use of integration of RTE. With the use of the spherical harmonics method, the spectral radiation intensity is presented in a series of spherical functions. In the first approximation of this method, P_1 , the following linear dependence is assumed [1]:

$$I_{\lambda}(\vec{r}, \vec{\Omega}) = \frac{1}{4\pi} [G_{\lambda}(\vec{r}) + 3\vec{\Omega} \vec{q}_{\lambda}(\vec{r})] \quad (4)$$

By multiplying Eq. (1) by $\vec{\Omega}$ and integrating it over a solid angle, one can find that the radiative flux is related to the irradiation by equation

$$\vec{q}_{\lambda} = -D\nabla G_{\lambda} \quad (5)$$

where $D = \frac{1}{3\beta_{tr}}$ is the spectral radiation diffusion coefficient, $\beta_{tr} = \alpha + \sigma_{tr}$ is the transport extinction coefficient, $\sigma_{tr} = \sigma \cdot (1 - \bar{\mu})$ is the transport scattering coefficient, $\bar{\mu}$ is the asymmetry factor of scattering introduced as follows:

$$\bar{\mu} = \frac{1}{4\pi} \int_{(4\pi)} I_{\lambda}(\vec{\Omega}' \cdot \vec{\Omega}) \Phi(\vec{\Omega}' \cdot \vec{\Omega}) d\vec{\Omega}' \quad (6)$$

Note that Eq. (5) is obtained for an arbitrary scattering function but it is the same as that for the transport approximation when this function is replaced by a sum of the isotropic component and the term describing the peak of forward scattering [1,12]:

$$\Phi(\mu_0) = (1 - \bar{\mu}) + 2\bar{\mu}\delta(1 - \mu_0) \quad (7)$$

where $\mu_0 = \vec{\Omega} \cdot \vec{\Omega}'$ is the cosine of the angle of scattering. It means that P_1 approximation is insensitive to details of the scattering function and the asymmetry factor of scattering is the only parameter of scattering anisotropy taken into account in this approach. The latter does not lead to considerable errors in radiative heat transfer calculations in the practically important case of multiple scattering [1,12].

Substituting Eq. (5) into the radiation energy balance (2) we obtain the nonhomogeneous modified Helmholtz equation for the spectral irradiation:

$$-\nabla(D\nabla G_{\lambda}) + \alpha G_{\lambda} = 4\pi\alpha_g I_b(T_g) \quad (8)$$

The Marshak boundary conditions are used to complete the P_1 boundary-value problem [1]. One can also proceed to the variational formulation of the problem when the solution yields the minimum of the following functional [1,5]:

$$\chi_{\lambda} = \int_V \left[\frac{D}{2} \nabla G_{\lambda} + \frac{\alpha}{2} G_{\lambda}^2 - 4\pi\alpha_g I_b(T_g) G_{\lambda} \right] dV + \int_A \frac{\varepsilon_w}{2(2 - \varepsilon_w)} \left[\frac{G_{\lambda}^2}{2} - 4\pi I_b(T_w) G_{\lambda} \right] dA \quad (9)$$

where T_w and ε_w are the temperature and hemispherical emissivity of boundary surfaces. The first integral in Eq. (9) corresponds to the differential Eq. (8), which is true in the computational region, whereas the second integral takes into account the conditions at the region boundary. The order of the differential operator in Eq.

(9) is reduced by one compared with Eq. (8). As a result, the local linear approximations of function G_{λ} in triangle finite elements are sufficient. The final-element method (FEM) [27,28] can be used to solve the variational problem for functional (8) as it was done in papers [9,17,29]. The FEM is very convenient because this method is flexible and applicable for computational regions of complex shape.

It should be recalled that the box spectral model with constant values of absorption coefficient in a set of spectral bands is used in the current version of the CFD code FireFOAM. According to this spectral model, the Planck function, $I_b(T)$, in Eq. (8) is replaced by the following integral:

$$F_{bj}(T) = \int_{\lambda_{1j}}^{\lambda_{2j}} I_b(T) d\lambda \quad (10)$$

As a result, the integral value of irradiation, G_j , for every band of number “j” is obtained instead of the spectral irradiation. A contribution of the spectral band to the divergence of the integral (over the spectrum) radiative flux is given by the following relation:

$$\nabla \vec{q}_j = 4\pi\alpha_{g,j} F_{bj}(T_g) - \alpha_j G_j \quad (11)$$

Let consider the computational data for CO₂ absorption band with wavelength boundaries of $\lambda_1 = 4.1494 \mu\text{m}$ and $\lambda_2 = 4.5851 \mu\text{m}$ for the model flame with temperature field shown in Fig. 1b. The absorption coefficient in this spectral band calculated with the box gas radiation model is plotted in Fig. 2.

The radial optical thickness, τ , of the hottest region of the flame without water droplets is easily estimated by multiplying the absorption coefficient, $\alpha_{g,j}$, by the geometrical thickness, Δr , of this thin region. The calculations carried out by the authors show that a value of τ that is much smaller than unity is obtained. It means that the upper estimate of the radiative heat losses based on the optically thin approximation may be applicable in this scenario specific to the initial development stage of the fire.

The non-uniform triangulation of the computational region, which includes the main part of the temperature field of Fig. 1b, is shown in Fig. 3. The left boundary of the region is the surface of the liquid fuel. The smaller areas of finite elements were made in the region of more optically dense medium. The total number of triangular elements is $2 \times 40 \times 40 = 3200$. As usually, the radial coordinates of all the nodes were increased by the first radial interval of the mesh to avoid the formal difficulties in numerical calculations near the axis [1]. The finite elements near the front of the developing flame should be relatively small (as it is shown in Fig. 3) because of an expected increase in extinction in this part of the flame containing numerous absorbing and scattering water droplets. Note that triangular elements at a small distance from the liquid fuel look not good because of a significant difference between the radial and axial dimensions of the triangles. However,

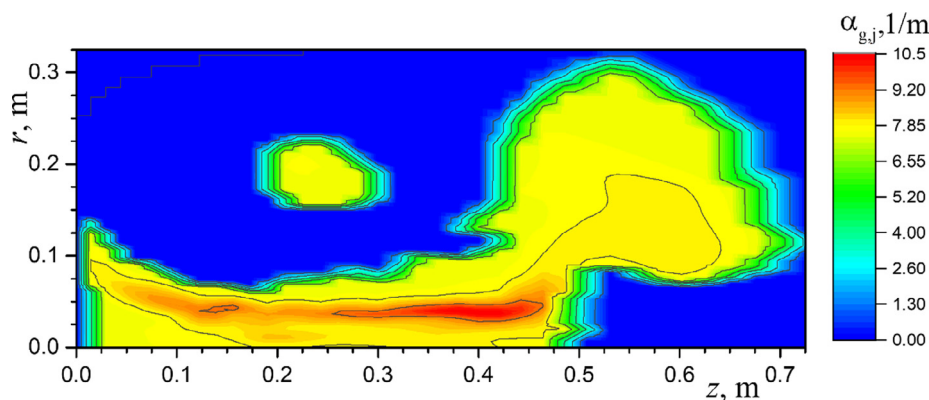


Fig. 2. Absorption coefficient calculated for the CO₂ absorption band.

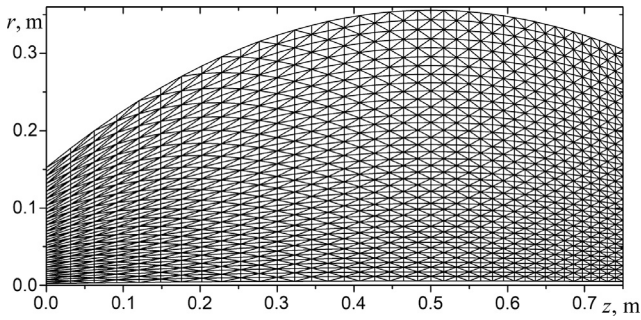


Fig. 3. Finite-element triangulation of the computational region.

additional calculations showed that this weakness is not critical in the case of the optically thin developing flame.

The following dimensionless function is calculated using various approaches:

$$\bar{W}_j = \frac{\nabla \vec{q}_j}{4\pi\alpha_{g,j}(T_{g,max})F_{b,j}(T_{g,max})} \quad (12)$$

This function is convenient to compare the results of calculations with those obtained in the optically thin limit when there is no need to solve the equations presented above because the following simplest relation is true for the radiative flux divergence [3,4]:

$$\nabla \vec{q}_j = 4\pi\alpha_{g,j}F_{b,j}(T_g) \quad (13)$$

The results of calculations are presented in Fig. 4. The FVM calculations are carried out using FireFoam. One can see that the difference

between the computational data obtained using the optically thin approximation, P_1 method, and FVM are similar to each other and the first of these approaches gives an upper estimate of radiative heat losses. The calculations based on P_1 and FVM give very close values of the radiative flux divergence, whereas the computational time of the P_1 calculations is about two orders of magnitude less than that of the regular FVM procedure used in the CFD code FireFoam. The results obtained confirm good accuracy of P_1 approximation which can be employed for very fast and reliable radiation calculations for the developing flames and can be recommended for implementation into any general CFD code. It should be recalled that P_1 is even more accurate in the case of a scattering medium [1] and can be used in radiative heat transfer calculations for the flames with water droplets as applied to the flame suppression problem.

The P_1 model is considered for calculations of the radiation term in the energy equation only. This is really important for the CFD flame calculations, but insufficient to determine the radiative flux outside the flame. Fortunately, the transport approximation can be employed to simplify the RTE, which can be written in the same way as that for isotropic scattering, i.e., with $\Phi = 1$ [1,5,12]:

$$\begin{aligned} \vec{\Omega} \nabla I_\lambda(\vec{r}, \vec{\Omega}) + \beta_{tr} I_\lambda(\vec{r}, \vec{\Omega}) &= S_\lambda(\vec{r}) - S_\lambda(\vec{r}) \\ &= \frac{\sigma_{tr}}{4\pi} G_\lambda(\vec{r}) + \alpha_g I_b(T_g) \end{aligned} \quad (14)$$

where S_λ is the so-called source function. The spectral radiation intensity can be calculated by direct integration of Eq. (14). This procedure is very simple in the case of an open flame when no radiation illuminates the flame surface and the formal solution along the ray \vec{s} is as follows:

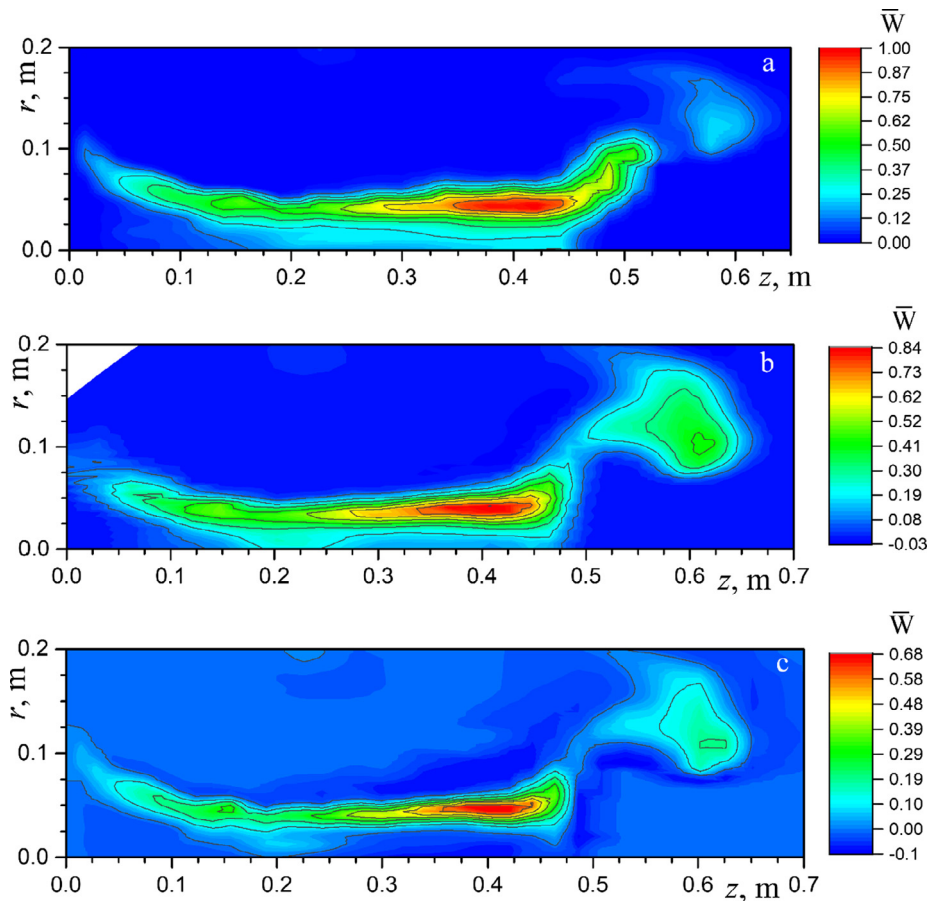


Fig. 4. The divergence of radiative flux in the CO₂ absorption band: a – optically thin approximation, b – P_1 calculation, c – FVM calculation.

$$I_i(s) = \int_0^s S_i(l) \exp \left[\int_0^l \beta_{tr}(l') dl' - \int_0^s \beta_{tr}(l') dl' \right] dl \quad (15)$$

Eq. (14) can be rewritten as applied to a set of spectral bands considered in the box model. In the combined two-step method of the present paper, the source function is calculated at the first step using of the P_1 solution for irradiation G_i . After that, a ray-tracing procedure for the transport RTE solution should be used at the second step to calculate accurately the radiative flux to an arbitrary surface outside the flame, if necessary. It is interesting that there is a potential possibility of comparison of computational predictions with experimental data for the radiation of pool fire flames [30].

4. Computational model for the probe stage of fire suppression

The effects of water sprays on the flow field parameters of the flame should be taken into account in computational studies for the regular developed regime of fire suppression, and this is an important engineering problem [31–34]. However, the problem is significantly simplified at the probe stage of fire suppression suggested in [22] because this preliminary stage of fire suppression is characterized by a very small flow rate of water. The observations at the probe stage could show us some details of behavior of evaporating water droplets in the flame.

A short-time probe stage of fire suppression is considered in the present paper. Therefore, the motion, heating, and evaporation of single droplets can be studied without account for any feedback effects. The radiative power absorbed by droplets is neglected because it is much less than the heat supplied to the droplets by convective heat transfer from hot combustion gases in the flame. In more detailed calculations, the effect of radiation can be taken into account as it was done in recent papers on shielding of fire radiation by water mists [35,36] and also in the problem of a space vehicle shielding from solar radiation by a cloud of sublimating particles [37].

The interaction of water sprays with fires has been modeled computationally in many papers during the last two decades [38–45], but there is no need to discuss here the state-of-the-art in this field because of the main focus on the radiative transfer problem. Of course, there is a size distribution of water droplets at the initial cross section of the spray. However, the assumption of independent behavior of droplets makes it possible to consider a set of solutions for droplets of different size in the expected range of the initial droplet size distribution. The trajectories of droplets moving along the flame axis are considered. The radial component of gas velocity in a flame is much less than the axial gas velocity. In addition, the initial direction of the droplet motion is also close to the axial one. This makes the 1-D approach for the dynamic and thermal interaction of water droplets and flame to be acceptable for the computational estimates of the main effects. To simplify the problem, we do not consider also the secondary effects of the vapor coming from evaporating droplets on both the drag force and convective heat flux to the droplet. This is the usual assumption used in computational models of this kind. The initial problem for the droplet motion is as follows [18,41,46]:

$$\frac{dz_d}{dt} = u_d \quad z_d(0) = z_0 \quad (16a)$$

$$\frac{du_d}{dt} = \frac{3C_D}{8a} \frac{\rho}{\rho_w} (u_g - u_d)|u_g - u_d| - g \quad u_d(0) = -u_{d0} \quad (16b)$$

$$C_D = \frac{24(1 + 0.15\text{Re}_d^{0.687})}{\text{Re}_d} \quad \text{Re}_d = 2\rho|u - u_d| \frac{a}{\eta} \quad (16c)$$

where the subscript “w” refers to water, u is the axial component of velocity, a is the droplet radius, C_D is the drag coefficient, Re is the Reynolds number. It is assumed that water droplets are first heated up to the saturation temperature:

$$\frac{dT_d}{dt} = \frac{1.5\text{Nu}k}{\rho_w c_w a^2} (T_g - T_d) \quad T_d(0) = T_0 \quad t < t_{\text{sat}} \quad (17a)$$

$$\text{Nu} = 2 + 0.6\text{Re}_d^{1/2} \text{Pr}^{1/3} \quad \text{Pr} = \frac{\eta C}{k} \quad (17b)$$

(Nu and Pr are the Nusselt and Prandtl numbers) and then evaporated according to the following equation:

$$\frac{da}{dt} = -\text{Nu} \frac{k(T_g - T_{w,\text{sat}})}{2a\rho_w L_w} \quad a(t_{\text{sat}}) = a_0 \quad t \geq t_{\text{sat}} \quad (18)$$

where L_w is the latent heat of evaporation of water. A similar model has been also used in papers [22,35,36]. This simplified evaporation model is also sufficient for qualitative estimates of the present paper because of very fast heating of moving droplets and large molar fraction of water vapour in the flame. It is not necessary at the moment to consider sophisticated evaporation models like that developed in paper [47]. A transfer from the droplet heating to its evaporation is given by the following simple equation:

$$T_d(t_{\text{sat}}) = T_{w,\text{sat}} \quad (19)$$

Obviously, the local relative volume fraction of water droplets can be calculated as:

$$\bar{f}_v = \frac{f_v}{f_{v0}} = \left(\frac{u_{d0}}{u_d} \right) \left(\frac{a}{a_0} \right)^3 \quad (20)$$

Let consider the axial profiles of a gas temperature, T_g , and velocity, u_g , on the axis of symmetry ($r = 0$) and also along the lines of $r = 0.05$ m, 0.1 m, and 0.15 m for the flame shown in Fig. 1b. The profiles plotted in Fig. 5 in a combination with temperature field presented in Fig. 1b makes clear a strong non-uniformity of the developing flame. A very hot narrow circular region in a vicinity of a ring with radius of $r = 0.05$ m and height between $z = 0.31$ m and 0.46 m (red curves in Fig. 5a and b) moves upward with a relatively high speed of about 4 m/s. At the same time, there is a relatively thick region of a cold and slowly moving gas near the flame axis at $z > 0.5$ m and $r < 0.08$ m. Moreover, a downward motion of a gas is observed in a part of this region. One can see that both the gas temperature and velocity profiles at $r = 0.1$ m and 0.15 m are quite different from those at $r = 0$ and 0.05 m. The above described specific structure of the flame is a motivation of subsequent attention to behaviour of water droplets moving in the flame along different axial lines.

Before proceeding to the computational modeling of motion of water droplets in a gas flow, it is interesting to estimate the so-called relaxation time, t_{rel} , of the droplets. This can be done on the basis of the Stokes law which is true in the case of $\text{Re}_d < 1$ [48]:

$$t_{\text{rel}} = \frac{2}{9} \frac{\rho a^2}{\eta} \quad (21)$$

Eq. (21) gives very small values of $t_{\text{rel}} < 0.25$ ms for water droplets of radius $a < 100$ μm . It means that water droplets should be supplied at a small axial distance from the flame and the initial velocity of droplets should be sufficient to reach a hot region inside the flame.

Obviously, the effect of initial conditions decreases along the droplet trajectory, and the equilibrium position of a droplet is characterized by the same absolute values of two opposite forces: the force of gravity and the drag force which supports the droplet. In the case of a relatively small evaporating droplet, this condition

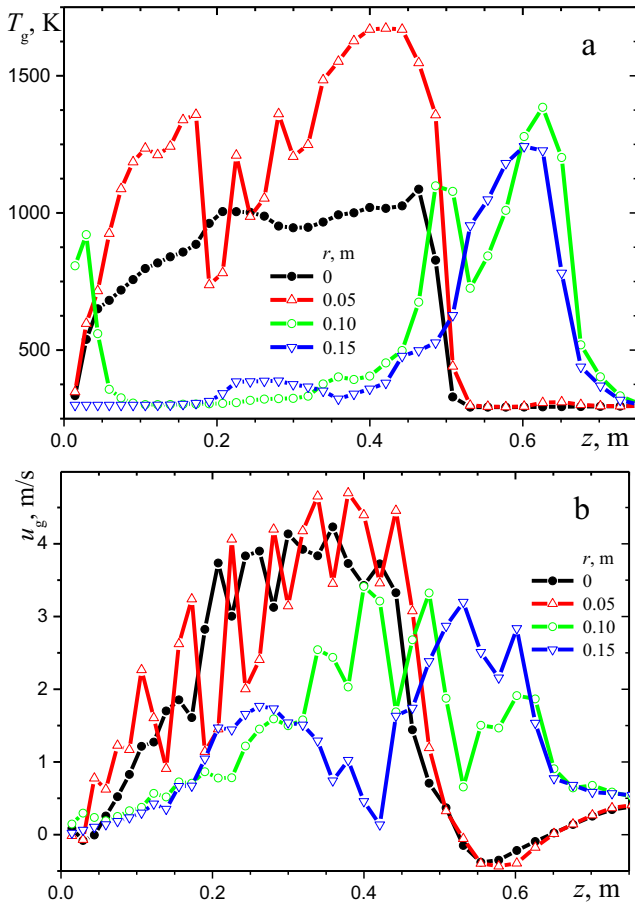


Fig. 5. The axial profiles of (a) temperature and (b) axial component of velocity of gaseous combustion products in the model flame.

can be written using the Stokes law. The resulting value of the gas axial velocity is as follows:

$$u_g = \frac{2}{9} \frac{\rho_w g a^2}{\eta} \quad (22)$$

Having substituted $\frac{\eta}{\rho_w} = 1.8 \times 10^{-8} \frac{s}{m^2}$ and $a = 40 \mu\text{m}$ to Eq. (22), we obtain $u_g \approx 0.2 \text{ m/s}$. One can see in Fig. 5b that this value of the axial velocity is observed near the flame axis at $z_{\text{eq}} = 0.52 \text{ m}$. It is interesting to compare this estimate with detailed numerical calculations.

The numerical results for the current radius of evaporating water droplets along their trajectories in the case of the droplet initial position of $z_0 = 0.75 \text{ m}$ and various distances, r_0 , from the flame axis are presented at the in Fig. 6. The same effect is observed at different values of r_0 : one can choose the value of u_0 and the range of a_0 to observe focusing of all the droplets in small local regions where the equilibrium condition (22) is satisfied. It should be noted that the above estimate of z_{eq} for the droplets moving along the flame axis ($r_0 = 0$) is in good agreement with the calculations shown in Fig. 6a. The calculations for droplets moving along the flame axis don't show their complete evaporation because of a cold gas area near the axis. This is a special case when the thermal radiation of a hot flame should be taken into account in calculations of the droplet evaporation. On the contrary, large water droplets supplied at $r_0 = 0.1 \text{ m}$ and $r_0 = 0.15 \text{ m}$ can penetrate into the hot region and these droplets are totally evaporated during their backward motion at a small distance from this hot region.

It is physically clear that the volume fraction of water droplets increases dramatically in the local regions of their collection and

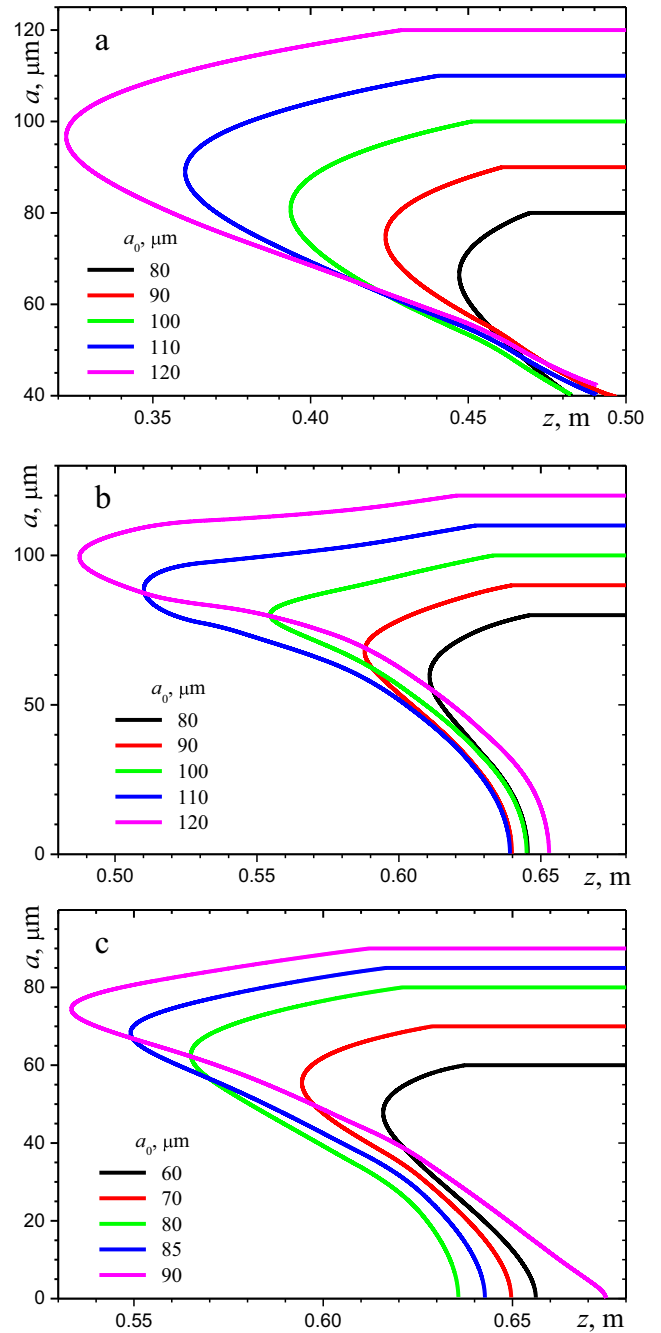


Fig. 6. Variation of radius of droplets along their trajectories at three initial positions of the droplets: (a) $r_0 = 0$ ($u_{d0} = 20 \text{ m/s}$), (b) $r_0 = 0.1 \text{ m}$ ($u_{d0} = 10 \text{ m/s}$), and (c) $r_0 = 0.15 \text{ m}$ ($u_{d0} = 15 \text{ m/s}$).

total evaporation. Strictly speaking, the assumption of independent motion of single droplets may be incorrect in the vicinity of these regions. However, following [20], this effect is not considered in the present paper.

5. Optical properties of water droplets

The normalized coefficients of absorption and transport scattering (per unit volume fraction of water) for independently absorbing and scattering droplets with radius a can be determined as follows:

$$E_a = 0.75 \frac{Q_a}{a} \quad E_s^{\text{tr}} = 0.75 \frac{Q_s^{\text{tr}}}{a} \quad (23)$$

According to Mie theory [49–51], the efficiency factors of absorption, Q_a , and transport scattering, Q_s^{tr} depend on both the complex index of refraction of water, $m = n - ik$, and diffraction parameter $x = \frac{2\pi a}{\lambda}$. The following approximate relations suggested in [52] are used in the calculations instead of the Mie theory:

$$Q_a = \frac{4n}{(n+1)^2} [1 - \exp(-4kx)] \quad Q_s^{\text{tr}} = K \cdot \begin{cases} \frac{\psi}{5} & \text{when } \psi \leq 5 \\ \left(\frac{\psi}{5}\right)^\gamma & \text{when } \psi > 5 \end{cases} \quad (24a)$$

$$K = 1.5n(n-1)\exp(-15k) \quad \gamma = 1.4 - \exp(-80k) \quad \psi = 2x(n-1) \quad (24b)$$

The spectral optical constants of water, n and k , can be found in early papers [53,54]. According to [55,56], we neglect a weak temperature dependence of the refractive index. It means that the most important value of transport scattering coefficient in the range of water semi-transparency can be calculated using the values of optical constants of water at room temperature. The calculated values of E_a and E_s^{tr} presented in Fig. 7 should be multiplied by the volume fraction of droplets to obtain the local values of the spectral absorption and transport scattering coefficients: $\alpha_d = f_v E_a$ and $\sigma_{\text{tr}} = f_v E_s^{\text{tr}}$. One can see that radiation absorption by water droplets is significant in the main near-infrared absorption band of water. It contributes to water evaporation and flame suppression. The scattering by small droplets is large over the spectrum excluding the absorption band, where the anomalous dispersion takes place [57,58]. The hypothesis of independent scattering does not work in the region of strong evaporation where the distance between the neighboring droplets may be comparable with the wavelength. The dependent scattering may lead to significant changes in optical properties of the medium [59–62]. However, this effect is a complex problem of physical optics and it is beyond the scope of the present paper. Therefore, the ordinary relations of independent scattering by single droplets are used in the estimates.

It should be noted that there are two serious assumptions of the suggested theoretical model and both of them are related with an expected high local volume fraction of small water droplets. Strictly speaking, one cannot consider independent motion of these

droplets and also independent scattering of infrared radiation by water droplets in some local regions of the flame. The resulting overall error of the simplified computational model depends strongly on water flow rate at the probe stage of the flame suppression. One can decrease this error in the experiments using additional probe-stage regimes with much lower flow rate of water.

6. Effect of radiation scattering by evaporating water droplets

The computational data presented in Fig. 7 confirm that the above choice of the representative CO₂ absorption band at wavelength about 4.3 μm will enable us to estimate the effect of scattering of the flame radiation by evaporating water droplets at the probe stage of fire suppression. Note that contributions of soot to both absorption and scattering of radiation are negligible in this spectral range [63–66]. The absorption of thermal radiation by droplets is very small in this range whereas the normalized transport scattering coefficient is very high: $E_s^{\text{tr}} = 300 \text{ cm}^{-1}$ at $a = 10 \mu\text{m}$ and $E_s^{\text{tr}} \approx 1000 \text{ cm}^{-1}$ at $a = 5 \mu\text{m}$ (see Fig. 7b). Following [67], the emissivity of the liquid fuel surface $\epsilon_w = 0.6$ was used in the calculations. The latter does not mean that thermal radiation of relatively cold liquid fuel is important. However, we take into account a partial reflection of the flame radiation from the surface of liquid fuel.

It was shown in the previous section of the paper that relatively small evaporating droplets of water are collected mainly at a small distance from the front of a developing flame. According to Eq. (20) the volume fraction, f_v , of slowly moving droplets in this thin region is very high and the absolute value of is directly proportional to the flow rate of water in water spray. The maximum value of $f_{v,\text{max}} = 10^{-3}$ and constant value of $E_s^{\text{tr}} = 800 \text{ cm}^{-1}$ are assumed for the cloud of droplets in subsequent calculations. To estimate the effect of infrared scattering by water droplets, the following analytical relations were used for the spatial variation of volume fraction of droplets near the flame with temperature field shown in Fig. 1b:

$$f_v = f_{v,\text{max}} \left[1 - \frac{\left(\frac{r}{r_{\text{max}}} - 1\right)^2}{2} \right] \exp \left[\xi \cdot \left(1 - \frac{z}{z_{\text{cl}}} \right) \right] \quad z_{\text{cl}} = z_{\text{min}} \varphi(r) \quad (25a)$$

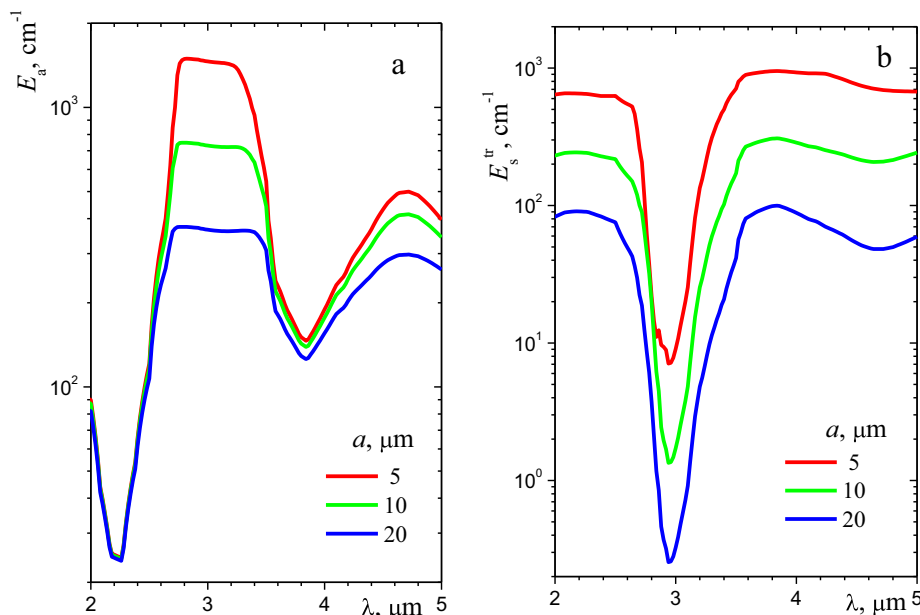


Fig. 7. Normalized (a) absorption and (b) transport scattering coefficients of water droplets.

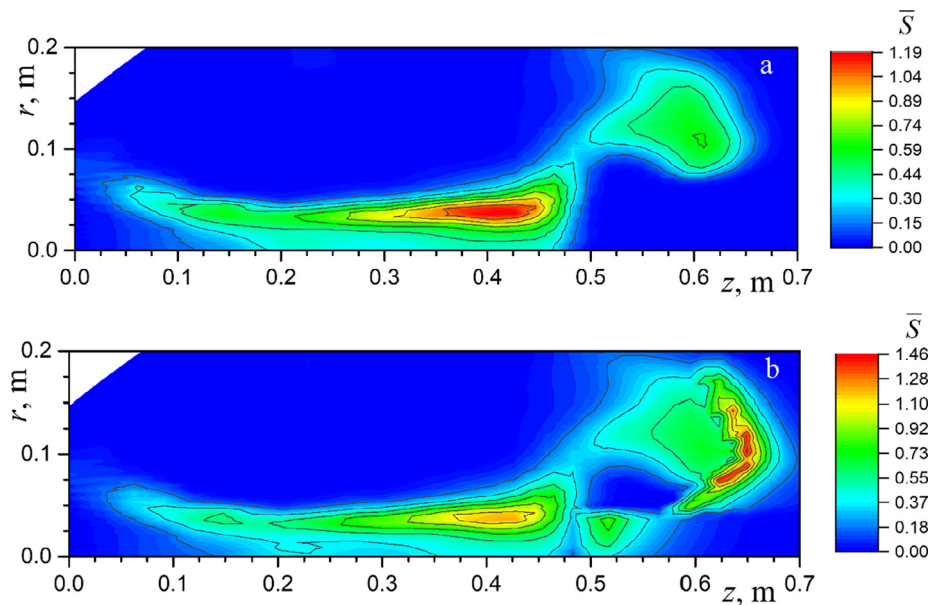


Fig. 8. The normalized radiative source function: a – without water droplets, b – with water droplets.

$$r_{\max} = 0.1 \text{ m} \quad \zeta = 10 \text{ m}^{-1} \quad z_{\min} = 0.5 \text{ m} \quad (25b)$$

$$\varphi(r) = \begin{cases} 1, & r < 0.05 \text{ m} \\ 1 + \zeta_1 r, & 0.05 \leq r < 0.1 \text{ m} \\ 1.4 - \zeta_2 r, & 0.1 \leq r < 0.2 \text{ m} \end{cases} \quad \zeta_1 = 3 \text{ m}^{-1} \quad \zeta_2 = 1 \text{ m}^{-1} \quad (25c)$$

It is assumed that scattering by water droplets in the region of $z < z_{cl}$ and also at $r > 0.2 \text{ m}$ is negligibly small.

As discussed above, the observed radiation from the flame is determined by the radiative source function. Therefore, the effect of infrared scattering by water droplets on the source function is considered. Following the above normalization, the source function for the transport RTE calculated using the P_1 solution for irradiation is divided by the maximum value of the source function calculated using the optically thin approximation. The finite-element triangulation of the computational region shown in Fig. 5 was used in the calculations. The resulting field of dimensionless value of \bar{S} calculated using P_1 approximation is presented in Fig. 8. One can see that a cloud of small evaporating droplets leads to significant changes in the field of radiative source function just in front of the developing flame. This effect is expected to be interesting for the infrared diagnostics of transient flames at the probe stage of fire suppression. The latter can be used for partial validation of CFD simulations. To the best of our knowledge, there is no appropriate data in the literature on infrared measurements of thermal radiation of a flame suppressed by a jet of water droplets. However, such an experimental work would be interesting.

7. Conclusions

A procedure based on the earlier developed combined two-step method is suggested to simplify time-consuming spectral radiative transfer calculations in transient pool fires during their suppression using water sprays. A comparison with the reference numerical solution indicates that the accuracy of the P_1 approximation used at the first step of the method is sufficient for the calculations of the radiative flux divergence. This will lead to a significant simplification of the radiative module in the CFD code and much faster

radiation calculations. This result can be considered as an important stage in improving the fire radiation modeling.

The calculations of motion, heating, and evaporation of water droplets at the probe stage of fire suppression indicated the local areas of focusing of moving droplets before their total evaporation in the flame. The effect of infrared radiation scattering by these small droplets on the source function responsible for the radiation from the flame is considerable. It is important that positions of the local highly-scattering areas are very sensitive to the flame parameters. This can be used in probe experiments for partial validation of transient CFD simulations.

Conflict of interests

None declared.

Acknowledgements

The authors gratefully acknowledge the financial support by the H2020-MSCA-IF-2016 Programme of the European Commission (RAD-FIRE project, no. 749220). We also wish to thank Antoine Hubert and Okorie Ukairo for their kind assistance in processing the pool fire data and formatting the paper.

Appendix A. Supplementary material

Supplementary data associated with this article can be found, in the online version, at <https://doi.org/10.1016/j.ijheatmasstransfer.2018.07.095>.

References

- [1] L.A. Dombrovsky, D. Baillis, *Thermal Radiation in Disperse Systems: An Engineering Approach*, Begell House, New York, 2010.
- [2] R. Viskanta, *Radiative Transfer in Combustion Systems: Fundamentals and Applications*, Begell House, New York, 2005.
- [3] J.R. Howell, R. Siegel, M.P. Mengüç, *Thermal Radiation Heat Transfer*, CRC Press, New York, 2010.
- [4] M.F. Modest, *Radiative Heat Transfer*, third edition., Acad. Press, New York, 2013.
- [5] L.A. Dombrovsky, Approximate methods for calculating radiation heat transfer in dispersed systems, *Therm. Eng.* 43 (3) (1996) 235–243.

- [6] V.M. Borisov, A.A. Ivankov, The P_1 and P_2 approximations of the spherical harmonic method as applied to radiative heat transfer computations with allowance for strong blowing from the surface of a vehicle moving in the Jovian atmosphere, *Comput. Math. & Math. Phys.* 46 (9) (2006) 1611–1622.
- [7] L.A. Dombrovsky, W. Lipiński, A. Steinfeld, A diffusion-based approximate model for radiation heat transfer in a solar thermochemical reactor, *J. Quant. Spectr. Radiat. Transfer* 103 (3) (2007) 601–610.
- [8] D.A. Kontogeorgos, E.P. Keramida, M.A. Founti, Assessment of simplified thermal radiation models for engineering calculations in natural gas-fired furnace, *Int. J. Heat Mass Transfer* 50 (25–26) (2007) 5260–5268.
- [9] T. Klason, X.S. Bai, M. Bahador, T.K. Nilsson, B. Sundén, Investigation of radiative heat transfer in fixed bed biomass furnaces, *Fuel* 87 (10–11) (2008) 2141–2153.
- [10] L.A. Dombrovsky, W. Lipiński, A combined P_1 and Monte Carlo model for multi-dimensional radiative transfer problems in scattering media, *Comput. Thermal Sci.* 2 (6) (2010) 549–560.
- [11] D.A. Andrienko, S.T. Surzhikov, P_1 approximation applied to the radiative heating of descent spacecraft, *J. Spacecraft Rockets* 49 (6) (2012) 1088–1098.
- [12] L.A. Dombrovsky, The use of transport approximation and diffusion-based models in radiative transfer calculations, *Comput. Therm. Sci.* 4 (4) (2012) 297–315.
- [13] L.A. Dombrovsky, V. Timchenko, M. Jackson, Indirect heating strategy of laser induced hyperthermia: an advanced thermal model, *Int. J. Heat Mass Transfer* 55 (17–18) (2012) 4688–4700.
- [14] D.A. Andrienko, S.T. Surzhikov, J.S. Shang, Spherical harmonics method applied to the multi-dimensional radiative transfer, *Comp. Phys. Commun.* 184 (10) (2013) 2287–2298.
- [15] J. Cai, C. Lei, A. Dasgupta, M.F. Modest, D.C. Haworth, High fidelity radiative heat transfer models for high-pressure laminar hydrogen-air diffusion flames, *Combust. Theory Model.* 18 (6) (2014) 607–626.
- [16] J. Cai, R. Marques, M.F. Modest, Comparisons of radiative heat transfer calculations in a jet diffusion flame using spherical harmonics and k-distributions, *ASME J. Heat Transfer* 136 (11) (2014), 112702-1–112702-9.
- [17] L.A. Dombrovsky, D.L. Reviznikov, A.V. Sposobin, Radiative heat transfer from supersonic flow with suspended particles to a blunt body, *Int. J. Heat Mass Transfer* 93 (2016) 853–861.
- [18] Y. Sun, X. Zhang, Contributions of gray gases in SLW for non-gray radiation heat transfer and corresponding accuracies of FVM and P_1 method, *Int. J. Heat Mass Transfer* 121 (2018) 819–831.
- [19] L.A. Dombrovsky, L.G. Barkova, Solving the two-dimensional problem of thermal-radiation transfer in an anisotropically scattering medium using the finite element method, *High Temp.* 24 (4) (1986) 585–592.
- [20] A.V. Kolpakov, L.A. Dombrovsky, S.T. Surzhikov, Transfer of directed radiation in an absorbing and anisotropically scattering medium, *High Temp.* 28 (5) (1990) 753–757.
- [21] L.A. Dombrovsky, Evaluation of the error of the P_1 approximation in calculations of thermal radiation transfer in optically inhomogeneous media, *High Temp.* 35 (4) (1997) 676–679.
- [22] L.A. Dombrovsky, S. Dembele, J.X. Wen, An infrared scattering by evaporating droplets at the initial stage of a pool fire suppression by water sprays, *Infrared Phys. Technol.* 91 (2018) 55–62.
- [23] I. Sikic, J.X. Wen, S. Dembele, Evaluation of different schemes of the weighted-sum-of-grey-gases model for fire simulations, in: *Proc. 9th US Nat. Combust. Meeting, Combust. Inst.*, 2015.
- [24] B.F. Magnussen, B.H. Hjertager, Development of the eddy-break-up model of turbulent combustion, *Proc. Combust. Inst.* 16 (1976) 719–729.
- [25] Z. Chen, J. Wen, B. Xu, S. Dembele, Large eddy simulation of a medium-scale methanol pool fire using the extended eddy dissipation concept, *Int. J. Heat Mass Transfer* 70 (2014) 389–408.
- [26] D.K. Edwards, Molecular gas radiation, *Advances in Heat Transfer* 12 (1976) 115–193.
- [27] Z. Chen, *The Finite Element Method: Its Fundamentals and Applications in Engineering*, World Sci. Publ, Singapore, 2011.
- [28] O.C. Zienkiewicz, R.L. Taylor, J.Z. Zhu, *The Finite Element Method: Its Basis and Fundamentals*, seventh ed., Elsevier, New York, 2013.
- [29] L.A. Dombrovsky, J.H. Randlealisoa, W. Lipiński, V. Timchenko, Simplified approaches to radiative transfer simulations in laser induced hyperthermia of superficial tumors, *Comput. Thermal Sci.* 5 (6) (2013) 521–530.
- [30] L. Zhou, D. Zeng, D. Li, M. Chaos, Total radiative heat loss and radiation distribution of liquid pool fire flames, *Fire Safety J.* 89 (2017) 16–21.
- [31] S. Dembele, V.H.Y. Tam, S. Ferrais, R.A.F. Rosario and J.X. Wen, Effectiveness of water deluge in fire suppression and mitigation, *ICHEME Symp. Series No. 153* (2007) 8 pp.
- [32] H.Z. Yu, Physical scaling of water mist suppression of pool fires in enclosures, *Fire Safety J.* 10 (2011) 145–158.
- [33] M. Gupta, A. Pasi, A. Ray, S.R. Kale, An experimental study of the effects of water mist characteristics on pool fire suppression, *Exper. Thermal Fluid Sci.* 44 (2013) 768–778.
- [34] A. Jenft, A. Collin, A. Boulet, G. Pianet, A. Breton, B.A. Muller, Experimental and numerical study of pool fire suppression using water mist, *Fire Safety J.* 67 (2014) 1–12.
- [35] L.A. Dombrovsky, S. Dembele, J.X. Wen, A simplified model for the shielding of fire thermal radiation by water mists, *Int. J. Heat Mass Transfer* 96 (2016) 199–209.
- [36] L.A. Dombrovsky, S. Dembele, J.X. Wen, Shielding of fire radiation with the use of multi-layered mist curtains: preliminary estimates, *Comput. Thermal Sci.* 8 (4) (2016) 371–380.
- [37] L.A. Dombrovsky, D.L. Reviznikov, A.P. Kryukov, V.Yu. Levashov, Self-generated clouds of micron-sized particles as a promising way of a solar probe shielding from intense thermal radiation of the Sun, *J. Quant. Spectr. Radiat. Transfer* 200 (2017) 234–243.
- [38] R. Alpert, Numerical modelling of the interaction between automatic sprinkler sprays and fire plumes, *Fire Safety J.* 9 (1985) 157–163.
- [39] B. Downie, C. Polymeropoulos, G. Godos, Interaction of a water mist buoyant methane diffusion flame, *Fire Safety J.* 24 (1995) 359–381.
- [40] K. Prasad, C. Liu, K. Kailasanath, Simulation of water mist suppression of small scale methanol liquid fires, *Fire Safety J.* 33 (1999) 185–212.
- [41] J. Hua, K. Kumar, B.C. Khoo, H. Xue, A numerical study of the interaction of water spray with fire plume, *Fire Safety J.* 37 (2002) 631–657.
- [42] M.-H. Feng, Q.-W. Li, J. Qin, Extinguishment of hydrogen diffusion flames by ultrafine water mist in a cup burner apparatus – a numerical study, *Int. J. Hydrogen Energy* 40 (2015) 13643–13652.
- [43] T. Beji, S.E. Zadeh, G. Maragkos, B. Merci, Influence of droplet size distribution and volume fraction angular distribution on the results and computational time of water spray CFD simulations, *Fire Safety J.* 91 (2017) 586–595.
- [44] J. Floid, R. McDermont, Development and evaluation of two new droplet evaporation schemes for fire dynamics simulations, *Fire Safety J.* 91 (2017) 643–652.
- [45] T. Beji, S. Ebrahimzadeh, G. Maragkos, B. Merci, Numerical modelling of the interaction between water sprays and hot air jets – Part II: Two-phase flow simulations, *Fire Safety J.* 96 (2018) 143–152.
- [46] C.T. Crowe, J.D. Schwarzkopf, M. Sommerfeld, Y. Tsuji, *Multiphase Flows with Droplets and Particles*, second ed., CRC Press, New York, 2011.
- [47] A.P. Kryukov, V.Yu. Levashov, I.N. Shishkova, Evaporation in mixture of vapour and gas mixture, *Int. J. Heat Mass Transfer* 52 (23–24) (2009) 5585–5590.
- [48] G. Falkovich, *Fluid Mechanics (A short course for physicists)*, Cambridge Univ. Press, Cambridge (UK), 2011.
- [49] H.C. van de Hulst, *Light Scattering by Small Particles*, Dover, New York, 1981.
- [50] C.F. Bohren, D.R. Huffman, *Absorption and Scattering of Light by Small Particles*, Wiley, New York, 1983.
- [51] W. Hergert, T. Wriedt, *The Mie Theory: Basics and Applications*, Springer, Berlin, 2012.
- [52] L.A. Dombrovsky, Spectral model of absorption and scattering of thermal radiation by diesel fuel droplets, *High Temp.* 40 (2) (2002) 242–248.
- [53] G.M. Hale, M.P. Query, Optical constants of water in the 200 nm to 200 μm wavelength region, *Appl. Optics* 12 (3) (1973) 555–563.
- [54] V.M. Zolotarev, A.V. Dyomin, Optical constants of water in wide wavelength range 0.1 μm –1m, *Optics Spectr.* 43 (2) (1977) 271–279.
- [55] J.B. Hawkes, R.W. Astheimer, The temperature coefficient of the refractive index of water, *J. Opt. Soc. Am.* 38 (9) (1948) 804–806.
- [56] A.N. Bashkatov, E.A. Genina, Water refractive index in dependence on temperature and wavelength: a simple approximation, in: *Proc. SPIE 5068* (2003) 393–395.
- [57] M. Born, E. Wolf, *Principles of Optics*, seventh (expanded) edition, Cambridge Univ. Press, New York, 1999.
- [58] M. Hancer, R.P. Sperline, J.D. Miller, Anomalous dispersion effects in the IR-ATR spectroscopy of water, *Appl. Spectr.* 54 (2000) 133–143.
- [59] M.I. Mishchenko, L.D. Travis, A.A. Lacis, *Multiple Scattering of Light by Particles: Radiative Transfer and Coherent Backscattering*, Cambridge Univ Press, Cambridge (UK), 2006.
- [60] Y. Okada, A.A. Kokhanovsky, Light scattering and absorption by densely packed groups of spherical particles, *J. Quant. Spectr. Radiat. Transfer* 110 (11) (2009) 902–917.
- [61] M.I. Mishchenko, *Electromagnetic Scattering by Particles and Particle Groups: An Introduction*, Cambridge Univ. Press, Cambridge (UK), 2014.
- [62] L.X. Ma, J.Y. Tan, J.M. Zhao, F.Q. Wang, C.A. Wang, Multiple and dependent scattering by densely packed discrete spheres: Comparison of radiative transfer and Maxwell theory, *J. Quant. Spectr. Radiat. Transfer* 187 (2017) 255–266.
- [63] K.A. Jensen, J.M. Suo-Anttila, L.G. Blevins, Measurement of soot morphology, chemistry, and optical properties in the visible and near-infrared spectrum in the flame zone and overfire region of large JP-8 pool fires, *Combust. Sci. Technol.* 179 (12) (2007) 2453–2487.
- [64] L. Liu, M.I. Mishchenko, W.P. Arnott, A study of radiative properties of fractal soot aggregates using the superposition T-matrix method, *J. Quant. Spectr. Radiat. Transfer* 109 (15) (2008) 2656–2663.
- [65] F. Liu, C. Wong, D. Snelling, G.J. Smallwood, Investigation of absorption and scattering properties of soot aggregates of different fractal dimension at 532 nm using RDG and GMM, *Aerosol Sci. Technol.* 47 (12) (2013) 1393–1405.
- [66] N. Doner, F. Liu, Impact of morphology on the radiative properties of fractal soot aggregates, *J. Quant. Spectr. Radiat. Transfer* 187 (2017) 10–19.
- [67] A.Yu. Snegirev, Statistical modelling of thermal radiation transfer in buoyant turbulent diffusion flames, *Combust. Flame* 136 (1–2) (2004) 51–71.